Published for SISSA by Springer

Received: *March 3, 2025*
Revised: *May 6, 2025*
Accepted: *May 18, 2025*
Published: *June 19, 2025*

Improved measurement of absolute branching fraction of the inclusive decay $\Lambda_c^+ \to K_S^0 X$

The BESIII collaboration

E-mail: besiii-publications@ihep.ac.cn

Abstract: By analyzing $4.5\,\mathrm{fb}^{-1}$ of e^+e^- collision data accumulated with the BESIII detector at center-of-mass energies ranging from 4599.53 MeV to 4698.82 MeV, we report the measurement of the absolute branching fraction (BF) of the inclusive decay $\Lambda_c^+ \to K_S^0 X$ using the double-tag technique. The result is $\mathcal{B}(\Lambda_c^+ \to K_S^0 X) = (10.9 \pm 0.2 \pm 0.1)\%$, where the first uncertainty is statistical and the second is systematic. This result indicates that there are still undiscovered decay channels containing K_S^0 in the final state with a combined BF of $(3.0 \pm 0.4)\%$. The BF of the inclusive decay $\Lambda_c^+ \to \overline{K}^0/K^0 X$ is calculated to be $\mathcal{B}(\Lambda_c^+ \to \overline{K}^0/K^0 X) = (21.8 \pm 0.4 \pm 0.2)\%$, The result is in agreement with the prediction of the statistical isospin model.

Keywords: Branching fraction, Charm Physics, e^+-e^- Experiments

ArXiv ePrint: 2502.20821

https://doi.org/10.1007/JHEP06(2025)194

JHEP06(2025)194

Contents

1 Introduction

Charmed baryons serve as an excellent laboratory for understanding the properties of quantum chromodynamics (QCD) in the context of a heavy quark coupling with two light quarks. The ground state, Λ_c^+, was first observed by the MARKII experiment in 1979 [1]. In recent years, the BESIII Collaboration has reported a series of absolute branching fractions (BFs) of exclusive decays of Λ_c^+ [2–14]. These provided significantly improved BF values for the known decay modes, and some new decay modes were also discovered. The sum of the observed and predicted BFs of Λ_c^+ is approximately 90% [15, 16]. The measurements of the BFs of the inclusive decays of Λ_c^+ are important for understanding its decay mechanisms and inferring the extent of the undiscovered decays.

The Cabibbo-favored (CF) decays are the dominant decay modes of Λ_c^+ [17, 18]. According to the statistical isospin model, the sum of the BFs of both observed and predicted CF decays of Λ_c^+ is $(83.2 \pm 4.9)\%$ [16], mainly involving Λ, Σ, Ξ and $\overline{K}^0$ in the final state. The inclusive BFs are useful for calibrating the CF transition amplitude for Λ_c^+ and are particularly essential for the determination of the Λ_c^+ lifetime [18, 19].

In 2014, the BESIII experiment accumulated e^+e^- collision data at the center-of-mass energy $\sqrt{s} = 4599.53\,\text{MeV}$ corresponding to an integrated luminosity of $(586.9 \pm 0.1 \pm 3.9)$ pb^{-1}, which initiated many studies on the inclusive decay of Λ_c^+ [20–22]. In 2020, the BF of $\Lambda_c^+ \to K_S^0 X$ was measured for the first time, giving the result $(9.9 \pm 0.6 \pm 0.4)\%$ [22], where X means all possible final state particles. The statistical isospin model estimates the total BF of exclusive Λ_c^+ decays containing $\overline{K}^0/K^0$ to be $(21.7 \pm 0.8)\%$, as presented in table 1. However, the summed BF of all observed exclusive Λ_c^+ decays containing $\overline{K}^0/K^0$ only accounts for a total of $(15.8 \pm 0.6)\%$. The determination of the absolute BF of $\Lambda_c^+ \to \overline{K}^0/K^0 X$ is an important input for the search for unmeasured decay modes of Λ_c^+ and for testing the BFs predicted by the statistical isospin model.

This paper presents an improved measurement of the absolute BF of the inclusive decay $\Lambda_c^+ \to K_S^0 X$. The measurement is based on e^+e^- collision data taken with the BESIII detector at center-of-mass energies between 4599.53 MeV and 4698.82 MeV, corresponding to a total integrated luminosity of $4.5\,\text{fb}^{-1}$ [23]. The energy points and corresponding

Mode	Value	Mode	Value
Observed BF		Predicted BF	
$p\overline{K}^0$	$(3.18 \pm 0.14)\%$	$n\overline{K}^0\pi^+\pi^0$	$(3.07 \pm 0.16)\%$
$p\overline{K}^0\pi^0$	$(3.92 \pm 0.24)\%$	$p\overline{K}^0\pi^0\pi^0$	$(1.36 \pm 0.07)\%$
$p\overline{K}^0\pi^+\pi^-$	$(3.18 \pm 0.22)\%$	$n\overline{K}^0\pi^+\pi^+\pi^-$	$(0.14 \pm 0.09)\%$
$n\overline{K}^0\pi^+$	$(3.64 \pm 0.50)\%$	$p\overline{K}^0\pi^+\pi^-\pi^0$	$(0.22 \pm 0.14)\%$
$p\overline{K}^0\eta$	$(0.88 \pm 0.06)\%$	$n\overline{K}^0\pi^+\pi^0\pi^0$	$(0.10 \pm 0.06)\%$
$\Lambda\overline{K}^0K^+$	$(0.56 \pm 0.11)\%$	$p\overline{K}^0\pi^0\pi^0\pi^0$	$(0.03 \pm 0.02)\%$
$\Sigma^+\phi, \phi \to K^0_L K^0_S$	$(0.13 \pm 0.02)\%$	$(\Sigma K)^+\overline{K}^0$	$(0.68 \pm 0.34)\%$
$\Sigma^+K^{*0}, K^{*0} \to K^0\pi^0$	$(1.16 \pm 0.33) \times 10^{-3}$	$\Xi^0 K^0\pi^+$	$(0.62 \pm 0.06)\%$
$p\overline{K}^0K^0$	$(9.40 \pm 0.72) \times 10^{-4}$		
Σ^+K^0	$(9.40 \pm 2.80) \times 10^{-4}$		
$p\phi, \phi \to K^0_L K^0_S$	$(3.59 \pm 0.47) \times 10^{-4}$		
Sum	$(15.8 \pm 0.6)\%$		$(6.2 \pm 0.4)\%$
Total		$(22.0 \pm 0.7)\%$	

Table 1. Observed and predicted BFs of CF exclusive Λ_c^+ decays containing $\overline{K}^0/K^0$ [15, 16], where the observed BFs are quoted from the Particle Data Group (PDG) [15] and the predicted BFs are from ref. [16] by the statistical isospin model. The BFs of the $\overline{K}^0/K^0$ decay modes are obtained by doubling the corresponding K^0_S decay modes. At present, there is no evidence for the possible difference between K^0_S and K^0_L production in charm baryon decay and this has been neglected in this paper.

$\sqrt{s}$ (MeV)	Luminosity (pb^{-1})
$4599.53 \pm 0.07 \pm 0.74$	$586.9 \pm 0.1 \pm 3.9$
$4611.86 \pm 0.12 \pm 0.32$	$103.8 \pm 0.1 \pm 0.6$
$4628.00 \pm 0.06 \pm 0.32$	$521.5 \pm 0.1 \pm 2.8$
$4640.91 \pm 0.06 \pm 0.38$	$552.4 \pm 0.1 \pm 2.9$
$4661.24 \pm 0.06 \pm 0.29$	$529.6 \pm 0.1 \pm 2.8$
$4681.92 \pm 0.08 \pm 0.29$	$1669.3 \pm 0.2 \pm 8.8$
$4698.82 \pm 0.10 \pm 0.39$	$536.4 \pm 0.1 \pm 2.8$

Table 2. Center-of-mass energies and corresponding luminosities for data samples used in this work.

luminosities are listed in table 2. These energies ensure the clean production of the charmed hyperon pairs without additional hadrons, which facilitates the application of the double-tag (DT) method, initially introduced by the MARKIII Collaboration [24, 25]. Utilizing this technique, we reconstruct the $\overline{\Lambda}_c^-$ baryon through one of the eleven tag modes ($\overline{p}K^0_S$, $\overline{p}K^+\pi^-$, $\overline{p}K^0_S\pi^0$, $\overline{p}K^0_S\pi^-\pi^+$, $\overline{p}K^+\pi^-\pi^0$, $\overline{\Lambda}\pi^-$, $\overline{\Lambda}\pi^-\pi^0$, $\overline{\Lambda}\pi^-\pi^+\pi^-$, $\overline{\Sigma}^0\pi^-$, $\overline{\Sigma}^-\pi^0$ and $\overline{\Sigma}^-\pi^-\pi^+$), called single-tag (ST) $\overline{\Lambda}_c^-$. Subsequently, we identify the K^0_S candidate by reconstructing a pair of oppositely charged tracks that recoil against the ST $\overline{\Lambda}_c^-$, thereby forming a DT candidate. Charge conjugation is always implied throughout this paper.

2 BESIII experiment and Monte Carlo simulation

The BESIII detector [26] records symmetric e^+e^- collisions provided by the BEPCII storage ring [27] in the center-of-mass energies range from 2.0 GeV to 4.95 GeV, with a peak luminosity of 1.1×10^{33} cm^{-2}s^{-1} achieved at a center-of-mass energy of $\sqrt{s} = 3.77$ GeV. The cylindrical core of the BESIII detector covers 93% of the full solid angle and comprises a helium-based multilayer drift chamber (MDC), a plastic scintillator time-of-flight system (TOF), and a CsI(Tl) electromagnetic calorimeter (EMC), which are all enclosed in a superconducting solenoidal magnet providing a 1.0 T magnetic field. The solenoid is supported by an octagonal flux-return yoke which is segmented into layers and instrumented with resistive plate counter modules for muon identification. The charged-particle momentum resolution at 1 GeV/c is 0.5%, and ionization energy loss dE/dx resolution is 6% for electrons from Bhabha scattering. The EMC measures photon energies with a resolution of 2.5% (5%) at 1 GeV in the barrel (end cap) region. The time resolution of TOF barrel region is 68 ps, while that in the end cap region was 110 ps. The end cap TOF system was updated in 2015 using multigap resistive plate chamber technology, providing a time resolution of 60 ps [28–30]. About 85% of the $\Lambda_c^+\overline{\Lambda}_c^-$ pairs are produced in data taken after this upgrade. More details can be found in refs. [26, 27].

High-statistics Monte Carlo (MC) simulated data samples produced with GEANT4-based [31, 32] software, which includes the geometric description of the BESIII detector and the detector response, are used to determine detection efficiencies and estimate backgrounds. The e^+e^- annihilation is simulated with the KKMC generator [33] incorporating the initial-state radiation (ISR) effects and the beam energy spread. The inclusive MC sample includes the $\Lambda_c^+\overline{\Lambda}_c^-$ events, $D_{(s)}^{(*)}$ production, ISR return to lower-mass ψ states, and continuum processes $e^+e^- \to q\bar{q}$ ($q = u, d, s$). All the known decay modes of charmed hadrons and charmonia are modeled with EVTGEN [34, 35] using BFs taken from the PDG [15], while the remaining unknown decays are modeled with LUNDCHARM [36]. In addition, exclusive DT signal MC events, where the $\overline{\Lambda}_c^-$ decays into the studied ST channels and the Λ_c^+ decays into K_S^0X, are used to determine the DT detection efficiencies. For the MC production of $\Lambda_c^+\overline{\Lambda}_c^-$, the Born cross sections are taken into account [23], and phase space generated Λ_c^+ decays are reweighted according to their observed distributions.

3 Event selection

Charged tracks detected in the MDC are required to be within a polar angle (θ) range of $|\cos\theta| < 0.93$, where θ is defined with respect to the z axis, which is the symmetry axis of the MDC. The distance of the closest approach of the track to the interaction point (IP) must be less than 10 cm along the z axis, and within 1 cm in the transverse plane of the z axis. Both the time-of-flight system and the specific ionization energy loss (dE/dx) in the MDC are used to determine the likelihoods $\mathcal{L}$ of different particle type hypotheses. Tracks are identified as protons when the particle identification (PID) determines this hypothesis to have the greatest likelihood ($\mathcal{L}(p) > \mathcal{L}(K)$ and $\mathcal{L}(p) > \mathcal{L}(\pi)$), while charged kaons and pions are identified based on comparing the likelihoods for the two hypotheses ($\mathcal{L}(K) > \mathcal{L}(\pi)$ or $\mathcal{L}(\pi) > \mathcal{L}(K)$). These criteria are not required for the tracks that are used to reconstruct K_S^0 or $\overline{\Lambda}$.

JHEP06(2025)194

Neutral showers are reconstructed in the EMC. Showers not associated with any charged track are identified as photon candidates if they satisfy two additional criteria: (1) an energy deposition in the EMC of $E_{\rm dep} > 25\,{\rm MeV}$ in the barrel region corresponding to the polar angle $|\cos\theta| < 0.8$, while $E_{\rm dep} > 50\,{\rm MeV}$ in the end-cap region corresponding to $0.86 < |\cos\theta| < 0.92$. (2) the EMC time difference from the event start time is required to be less than 700 ns to suppress electronic noise and showers unrelated to the event. The π^0 candidates are reconstructed from photon pairs with the requirement that their invariant masses lie within $115\ {\rm MeV}/c^2 < M(\gamma\gamma) < 150\,{\rm MeV}/c^2$. To improve the momentum resolution, a mass-constrained kinematic fit to the π^0 nominal mass is applied to the photon pairs, and the updated energy and momentum of the π^0 are used for the further analysis.

Candidates for K_S^0 and $\overline{\Lambda}$ are formed by combining two oppositely charged tracks into the final states $\pi^+\pi^-$ and $\overline{p}\pi^+$. For these two tracks, their distances of closest approaches to the IP must be within $\pm 20\,{\rm cm}$ along the beam direction. No distance constraints in the transverse plane are required. The charged pion candidate is not subjected to the PID requirements described above, while PID for the proton is implemented to improve the quality of the signal. The two daughter tracks are constrained to originate from a common decay vertex, and the χ^2 of the vertex fit is required to be less than 100. Furthermore, the decay vertex is required to be separated from the IP by a distance of at least twice the fitted vertex resolution. The fitted momenta of the $\pi^+\pi^-$ and $\overline{p}\pi^+$ are used in the further analysis. To select K_S^0 and $\overline{\Lambda}$ candidates, we impose the requirements $487\ {\rm MeV}/c^2 < M(\pi^+\pi^-) < 511\ {\rm MeV}/c^2$ and $1111\ {\rm MeV}/c^2 < M(\overline{p}\pi^+) < 1121\ {\rm MeV}/c^2$, respectively, which are within about three standard deviations of their mass resolutions in the MC samples. The $\overline{\Sigma}^0$ and $\overline{\Sigma}^-$ candidates are reconstructed with $\gamma\overline{\Lambda}$ and $\overline{p}\pi^0$ with invariant masses in $1179\ {\rm MeV}/c^2 < M(\gamma\overline{\Lambda}) < 1203\,{\rm MeV}/c^2$ and $1176\ {\rm MeV}/c^2 < M(\overline{p}\pi^0) < 1200\,{\rm MeV}/c^2$, respectively.

For the tag modes $\overline{p}K_S^0\pi^0$, $\overline{p}K_S^0\pi^-\pi^+$, and $\overline{\Sigma}^-\pi^-\pi^+$, possible backgrounds with $\overline{\Lambda}\to\overline{p}\pi^+$ are rejected by requiring $M(\overline{p}\pi^+)$ outside the range $(1110, 1120)\,{\rm MeV}/c^2$. In addition, in the mode $\overline{p}K_S^0\pi^0$, candidate events within the range $1170\ {\rm MeV}/c^2 < M(\overline{p}\pi^0) < 1200\,{\rm MeV}/c^2$ are excluded to suppress $\overline{\Sigma}^-$ background. To remove K_S^0 candidates in the modes $\overline{\Lambda}\pi^-\pi^+\pi^-$, $\overline{\Sigma}^-\pi^0$, and $\overline{\Sigma}^-\pi^-\pi^+$, the invariant masses of $\pi^+\pi^-$ and $\pi^0\pi^0$ pairs are not allowed to fall in the range $(480, 520)\,{\rm MeV}/c^2$. The MC simulations show that peaking backgrounds and cross-feeds among the eleven tag modes are negligible after performing the above veto procedures.

The ST $\overline{\Lambda}_c^-$ yields are identified using the beam-constrained mass

$$M_{\rm BC} \equiv \sqrt{E^2_{\rm beam}/c^4 - |\vec{p}|^2/c^2}, \tag{3.1}$$

where $E_{\rm beam}$ is the value of the e^+ and e^- beam energies and $\vec{p}$ is the measured $\overline{\Lambda}_c^-$ momentum in the center-of-mass system of the e^+e^- collision. To improve the signal purity, the energy difference $\Delta E \equiv E - E_{\rm beam}$ for the $\overline{\Lambda}_c^-$ candidate is required to comply with a mode-dependent ΔE requirement, listed in table 3. Here, E is the total reconstructed energy of the $\overline{\Lambda}_c^-$ candidate. If more than one candidate satisfies the above requirements for each ST mode, we select the one with the minimum $|\Delta E|$. Unbinned maximum likelihood fits are performed on these $M_{\rm BC}$ distributions to obtain the ST yields, where the signal shapes are modeled with MC-simulated shapes convolved with Gaussian functions representing the resolution difference between data and MC simulation. The background shapes are described by an ARGUS function [37].

Tag mode	ΔE (MeV)
$\overline{\Lambda}_c^- \to \bar{p} K_S^0$	$(-21, 18)$
$\overline{\Lambda}_c^- \to \bar{p} K^+ \pi^-$	$(-29, 26)$
$\overline{\Lambda}_c^- \to \bar{p} K_S^0 \pi^0$	$(-49, 34)$
$\overline{\Lambda}_c^- \to \bar{p} K_S^0 \pi^- \pi^+$	$(-34, 31)$
$\overline{\Lambda}_c^- \to \bar{p} K^+ \pi^- \pi^0$	$(-60, 41)$
$\overline{\Lambda}_c^- \to \overline{\Lambda} \pi^-$	$(-23, 21)$
$\overline{\Lambda}_c^- \to \overline{\Lambda} \pi^- \pi^0$	$(-50, 41)$
$\overline{\Lambda}_c^- \to \overline{\Lambda} \pi^- \pi^+ \pi^-$	$(-40, 36)$
$\overline{\Lambda}_c^- \to \overline{\Sigma}^0 \pi^-$	$(-33, 31)$
$\overline{\Lambda}_c^- \to \overline{\Sigma}^- \pi^0$	$(-67, 32)$
$\overline{\Lambda}_c^- \to \overline{\Sigma}^- \pi^- \pi^+$	$(-40, 32)$

Table 3. The ΔE requirement for each tag mode.

On the DT side, the K_S^0 candidates are reconstructed from the remaining tracks on the recoiling side of the tagged $\overline{\Lambda}_c^-$. The K_S^0 selection criteria are the same as those used in the ST $\overline{\Lambda}_c^-$ selection. If there is more than one K_S^0 candidate, the one with the maximum L/σ_L, where L and σ_L are the K_S^0 decay length from the fit and its associated uncertainty, is selected for further analysis.

4 Measurement for branching fraction

A two-dimensional (2D) unbinned maximum likelihood fit to the distributions of $M_{\rm BC}$ versus the invariant mass of $\pi^+\pi^-$, $M(\pi^+\pi^-)$, is performed at the seven energy points simultaneously to determine the DT signal yields, with the results at $\sqrt{s} = 4681.92\,\text{MeV}$ shown in figure 1.

To obtain clean DT signal shapes, a match based on the MC truth information is performed for signal processes in the inclusive MC sample. The ratio to evaluate the quality of the match is defined as:

$$R_{d\vec{p}} = \frac{|\vec{p}_{\rm truth} - \vec{p}_{\rm rec}|}{|\vec{p}_{\rm truth}|}, \tag{4.1}$$

where $\vec{p}_{\rm truth}$ and $\vec{p}_{\rm rec}$ are the truth and reconstructed three-momenta of $\pi^\pm$. For matched events, the $\pi^+\pi^-$ from K_S^0 in the DT side are required to satisfy $R_{d\vec{p}}(\pi^+) < 0.5$ and $R_{d\vec{p}}(\pi^-) < 0.5$ in signal processes. Otherwise, they are defined as unmatched events. This match process will bring an efficiency, which is embeded in the DT efficiencies.

The DT signal shapes are described by the MC-simulated shapes of matched events convolved with Gaussian functions, whose parameters are free, while unmatched events have their own shapes. In the fit, the ratios of matched signal events and unmatched events are fixed based on a study of the signal processes in the inclusive MC samples.

JHEP06(2025)194

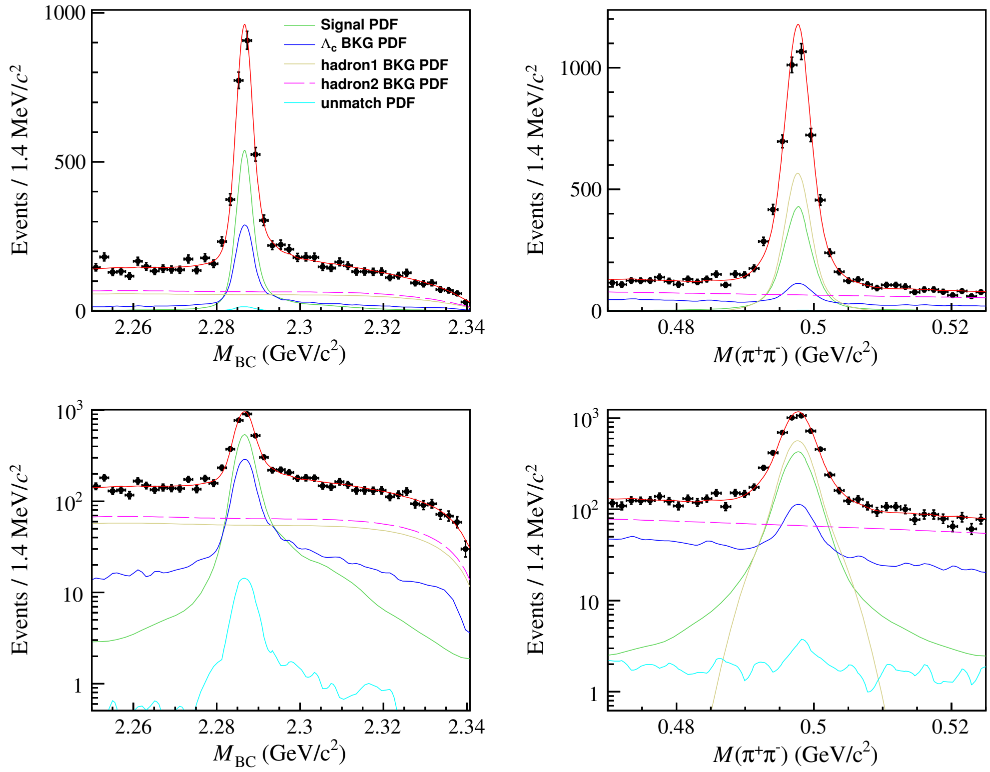

Figure 1. Projections of the simultaneous 2D fit to the $M_{\rm BC}$ versus $M(\pi^+\pi^-)$ distribution at $\sqrt{s} = 4681.92\,\mathrm{MeV}$. The points with error bars are data, the red solid lines are the sums of the fit functions, the green solid lines are the $\Lambda_c^+ \to K_S^0 X$ matched signal shapes, the blue solid lines are the $\Lambda_c^+\overline{\Lambda}_c^-$ background shapes, the brown solid lines are the hadron1 background shapes, the pink dashed lines are the hadron2 background shapes, and the cyan solid lines are the unmatched event shapes. The ordinate of the plots in the second row is logarithmic.

The background shapes from non-signal $e^+e^- \to \Lambda_c^+\overline{\Lambda}_c^-$ events are obtained from inclusive MC samples. The background from $e^+e^- \to q\bar{q}$ is divided into two types: peaking and combinatorial backgrounds in the $M(\pi^+\pi^-)$ distribution, named hadron1 and hadron2, respectively. Hadron1 is described by a third-order Chebyshev polynomial function in the $M_{\rm BC}$ distribution and a double Gaussian function in the $M(\pi^+\pi^-)$ distribution. Hadron2 is described by a third-order Chebyshev polynomial function in the $M_{\rm BC}$ distribution and a first-order Chebyshev polynomial function in the $M(\pi^+\pi^-)$ distribution. The parameters of these functions are obtained by performing a 2D unbinned maximum likelihood fit to the distribution of $M_{\rm BC}$ versus $M(\pi^+\pi^-)$ of $e^+e^- \to q\bar{q}$ MC samples. The yields of hadron1 and hadron2 are free parameters.

The BF of $\Lambda_c^+ \to K_S^0 X$ at the individual energy points can be obtained from the relative yields of DT events to ST events with the correction of their efficiencies estimated from MC simulations, which is given by:

$$\mathcal{B}_\alpha = \frac{N_\alpha^{\rm DT}}{\mathcal{B}_{\rm int} \cdot \sum_i \left(\frac{N_i^{\alpha,\rm ST}}{\varepsilon_i^{\alpha,\rm ST}} \cdot \varepsilon_i^{\alpha,\rm DT} \right)}, \tag{4.2}$$

JHEP06(2025)194

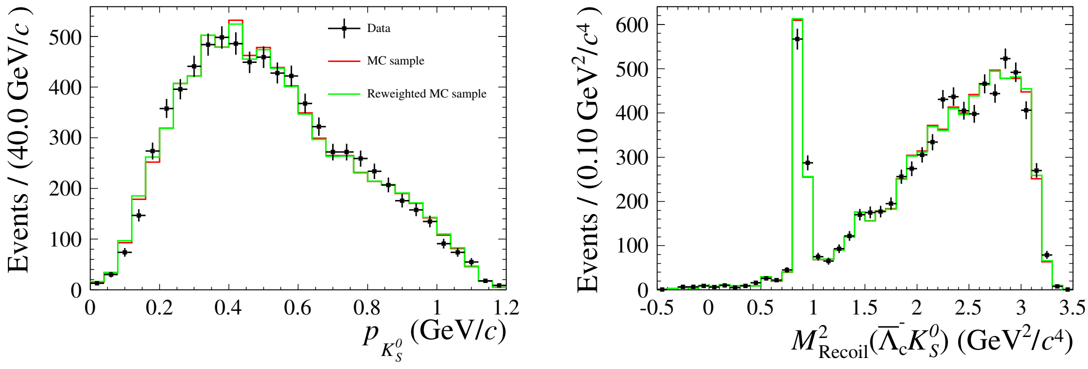

(a) (b)

Figure 2. The distributions of (a) $p_{K_S^0}$ and (b) $M^2_{\rm Recoil}(\bar{\Lambda}_c^- K_S^0)$ of the accepted candidates. The points with error bars are data, the solid red line is MC sample, the solid green line is reweighted MC sample. They are normalized according to the data.

where $N_\alpha^{\rm DT}$ is the DT yield, $\mathcal{B}_{\rm int}$ is the BF of $K_S^0 \to \pi^+\pi^-$ [15], $N_i^{\alpha,\rm ST}$ is the ST yield and $\varepsilon_i^{\alpha,\rm ST}$ is the ST efficiency, $\varepsilon_i^{\alpha,\rm DT}$ is the DT efficiency estimated by DT signal MC samples, i represents the index of each tag mode, and α stands for the label of the energy point.

However, we want to determine the overall BF of $\Lambda_c^+ \to K_S^0 X$, so we treat the BF as a shared parameter between energy points in the simultaneous fit and parametrize $N_\alpha^{\rm DT}$ in the fit as

$$N_\alpha^{\rm DT} \to \mathcal{B}_{\rm int} \cdot \sum_i \left(\frac{N_i^{\alpha,\rm ST}}{\varepsilon_i^{\alpha,\rm ST}} \cdot \varepsilon_i^{\alpha,\rm DT} \right) \cdot \mathcal{B}(\Lambda_c^+ \to K_S^0 X), \tag{4.3}$$

and the fit obtains $\mathcal{B}(\Lambda_c^+ \to K_S^0 X)$ directly.

To obtain a more accurate DT efficiency, we use the control sample $J/\psi \to K_S^0 K^\pm \pi^\mp$ to study the K_S^0 reconstruction efficiency. A factor depending on the K_S^0 momentum distribution is obtained by studying the difference of K_S^0 reconstruction efficiency between data and MC samples of $J/\psi \to K_S^0 K^\pm \pi^\mp$. We use this factor to weight the DT signal MC samples according to the K_S^0 momentum distribution in $\Lambda_c^+ \to K_S^0 X$. The relative difference between the corrected efficiencies and the uncorrected is $(1.8 \pm 0.3)\%$. Figure 2 shows the comparisons of the momentum of the K_S^0 candidate and the recoil mass square of the $\bar{\Lambda}_c^- K_S^0$ system, $M^2_{\rm Recoil}(\bar{\Lambda}_c^- K_S^0)$, where a clear peak of proton can be found. Good agreement between data and MC simulation can be seen.

The determination of ST yields and ST efficiencies are the same as in ref. [23]. The DT efficiencies of matched events are listed in table 4, and the fitted DT signal yields of $\Lambda_c^+ \to K_S^0 X$ at the seven energy points are listed in table 5. Finally, the BF of $\Lambda_c^+ \to K_S^0 X$ is determined to be $(10.9 \pm 0.2)\%$, where the uncertainty is statistical only. To verify this value is stable, we measured the BFs at different energy points combining all tag modes, listed in table 6. And the BFs at each tag mode combining all energy points samples, listed in table 7.

$\varepsilon_i^{\alpha,\mathrm{DT}}(\%)$	4599.53 MeV	4611.86 MeV	4628.00 MeV	4640.91 MeV	4661.24 MeV	4681.92 MeV	4698.82 MeV
$\overline{\Lambda}_c^- \to \bar{p}K_S^0$	32.5 ± 0.5	30.0 ± 1.2	29.1 ± 0.5	28.1 ± 0.5	28.5 ± 0.5	26.8 ± 0.3	25.0 ± 0.5
$\overline{\Lambda}_c^- \to \bar{p}K^+\pi^-$	29.1 ± 0.2	28.1 ± 0.5	26.8 ± 0.2	26.8 ± 0.2	26.2 ± 0.2	25.7 ± 0.1	25.2 ± 0.2
$\overline{\Lambda}_c^- \to \bar{p}K_S^0\pi^0$	12.5 ± 0.3	12.6 ± 0.8	11.0 ± 0.3	11.1 ± 0.3	10.7 ± 0.3	10.5 ± 0.2	10.6 ± 0.3
$\overline{\Lambda}_c^- \to \bar{p}K_S^0\pi^-\pi^+$	12.2 ± 0.3	11.2 ± 0.6	10.9 ± 0.3	11.0 ± 0.3	10.7 ± 0.3	10.6 ± 0.2	10.1 ± 0.3
$\overline{\Lambda}_c^- \to \bar{p}K^+\pi^-\pi^0$	11.1 ± 0.2	10.3 ± 0.4	9.5 ± 0.2	9.4 ± 0.2	9.4 ± 0.2	8.9 ± 0.1	9.3 ± 0.2
$\overline{\Lambda}_c^- \to \overline{\Lambda}\pi^-$	26.6 ± 0.6	27.8 ± 1.4	23.4 ± 0.6	22.7 ± 0.5	22.6 ± 0.6	22.8 ± 0.3	21.6 ± 0.6
$\overline{\Lambda}_c^- \to \overline{\Lambda}\pi^-\pi^0$	12.2 ± 0.2	10.7 ± 0.4	10.3 ± 0.2	10.5 ± 0.2	10.2 ± 0.2	9.7 ± 0.1	9.4 ± 0.2
$\overline{\Lambda}_c^- \to \overline{\Lambda}\pi^-\pi^+\pi^-$	7.9 ± 0.2	7.2 ± 0.5	7.3 ± 0.2	7.6 ± 0.2	7.4 ± 0.2	7.2 ± 0.1	7.3 ± 0.2
$\overline{\Lambda}_c^- \to \overline{\Sigma}^0\pi^-$	16.2 ± 0.5	15.7 ± 1.1	15.0 ± 0.5	15.1 ± 0.5	13.6 ± 0.5	14.8 ± 0.3	13.4 ± 0.5
$\overline{\Lambda}_c^- \to \overline{\Sigma}^-\pi^0$	13.5 ± 0.5	12.2 ± 1.1	13.3 ± 0.5	13.8 ± 0.5	12.5 ± 0.5	12.1 ± 0.3	11.0 ± 0.5
$\overline{\Lambda}_c^- \to \overline{\Sigma}^-\pi^-\pi^+$	14.2 ± 0.3	14.4 ± 0.6	13.4 ± 0.3	13.3 ± 0.3	12.4 ± 0.3	12.8 ± 0.2	12.4 ± 0.3

Table 4. The DT efficiencies of matched events $\varepsilon_i^{\alpha,\mathrm{DT}}$ for each tag mode at various energy points, where the uncertainties are statistical only.

$\sqrt{s}$ (MeV)	N_α^{DT}
4599.53	669 ± 38
4611.86	132 ± 17
4628.00	602 ± 36
4640.91	605 ± 36
4661.24	691 ± 39
4681.92	1733 ± 62
4698.82	507 ± 33
Total	4939 ± 104

Table 5. The fitted DT yields N_α^{DT} at various energy points.

$\sqrt{s}$ (MeV)	$\mathcal{B}(\Lambda_c^+ \to K_S^0 X)(\%)$
4599.53	10.0 ± 0.6
4611.86	11.3 ± 1.4
4628.00	11.0 ± 0.7
4640.91	11.0 ± 0.6
4661.24	11.2 ± 0.7
4681.92	10.9 ± 0.4
4698.82	11.1 ± 0.7
Total	10.9 ± 0.2

Table 6. The BFs at various energy points.

JHEP06(2025)194

Tag mode	$\mathcal{B}(\Lambda_c^+ \to K_S^0 X)(\%)$
$\overline{\Lambda}_c^- \to \bar{p} K_S^0$	11.1 ± 0.8
$\overline{\Lambda}_c^- \to \bar{p} K^+ \pi^-$	10.9 ± 0.4
$\overline{\Lambda}_c^- \to \bar{p} K_S^0 \pi^0$	11.3 ± 1.1
$\overline{\Lambda}_c^- \to \bar{p} K_S^0 \pi^- \pi^+$	10.9 ± 1.2
$\overline{\Lambda}_c^- \to \bar{p} K^+ \pi^- \pi^0$	10.7 ± 0.7
$\overline{\Lambda}_c^- \to \overline{\Lambda} \pi^-$	10.8 ± 1.0
$\overline{\Lambda}_c^- \to \overline{\Lambda} \pi^- \pi^0$	10.8 ± 0.7
$\overline{\Lambda}_c^- \to \overline{\Lambda} \pi^- \pi^+ \pi^-$	11.2 ± 1.0
$\overline{\Lambda}_c^- \to \overline{\Sigma}^0 \pi^-$	11.3 ± 1.3
$\overline{\Lambda}_c^- \to \overline{\Sigma}^- \pi^0$	10.9 ± 1.6
$\overline{\Lambda}_c^- \to \overline{\Sigma}^- \pi^- \pi^+$	10.8 ± 0.8
Total	10.9 ± 0.2

Table 7. The BFs at various tag modes.

5 Systematic uncertainty

The systematic uncertainties arising from the ST side mostly cancel in the BF measurement according to eq. (4.2). The systematic uncertainties from various sources are summarized in table 8 and discussed below.

- K_S^0 reconstruction.

  As described in section 4, $J/\psi \to K_S^0 K^\pm \pi^\mp$ decay is used as a control sample to determine the correction to the DT efficiencies of $(1.8 \pm 0.3)\%$. The systematic uncertainty in the K_S^0 reconstruction is 0.3%.

- 2D fitting. The uncertainty arising from the simultaneous 2D fitting is estimated by convolving the signal MC shape with a double Gaussian function to vary the signal shape, while the background from $e^+e^- \to q\bar{q}$ is described using the shape extracted from $e^+e^- \to q\bar{q}$ MC samples. The total uncertainty from the 2D fitting is 0.9%.

- Intermediate BF. The BF of $K_S^0 \to \pi^+\pi^-$, $\mathcal{B}_{\rm int} = (69.20 \pm 0.05)\%$ [15], gives an uncertainty of 0.1%.

- MC statistics. The statistical uncertainties of ST efficiencies and DT efficiencies are propagated to the BFs of signal channel according to eq. (4.2), and contribute with an uncertainty of 0.3%.

- ST $\overline{\Lambda}_c^-$ yield. The systematic uncertainty in the total ST yield arises from the background fluctuation together with a component coming from the fit to the $M_{\rm BC}$ distribution. It is studied by varying the parameters of signal shape, fitting range and endpoint of the ARGUS function, and then redoing the fit process. This gives an uncertainty of 0.4%.

JHEP06(2025)194

Source	$\Lambda_c^+ \to K_S^0 X$ (%)
K_S^0 reconstruction	0.3
2D fitting	0.9
Intermediate BF	0.1
MC statistics	0.3
ST $\overline{\Lambda}_c^-$ yield	0.4
$R_{d\bar{p}}$ requirement	0.1
Total	1.1

Table 8. Relative systematic uncertainties for the measured BF.

- $R_{d\bar{p}}$ requirement. The uncertainty arising from the $R_{d\bar{p}}$ is estimated by obtaining the BF without this requirement, leading to an uncertainty of 0.1%.

The total systematic uncertainty is 1.1% by summing all the uncertainties in quadrature, assuming no correlation exists between these sources.

6 Summary

The absolute BF of $\Lambda_c^+ \to K_S^0 X$ is measured based on about $4.5\,\mathrm{fb}^{-1}$ of e^+e^- collision data collected at center-of-mass energies ranging from 4599.56 MeV to 4698.82 MeV with the BESIII detector. The result is $\mathcal{B}(\Lambda_c^+ \to K_S^0 X) = (10.9 \pm 0.2 \pm 0.1)\%$, where the first uncertainty is statistical and the second is systematic. The precision of the measured BF is improved by a factor of three compared to the previous BESIII measurement $\mathcal{B}(\Lambda_c^+ \to K_S^0 X) = (9.9 \pm 0.6 \pm 0.4)\%$ [22]. Compared to the summed BF of the observed exclusive Λ_c^+ decays, $(7.9 \pm 0.3)\%$, our result indicates that the combined BF of the undiscovered decay channels of Λ_c^+ that include a K_S^0 meson in the final state is $(3.0 \pm 0.4)\%$. The BF of the inclusive decay $\Lambda_c^+ \to \overline{K}^0/K^0 X$ is calculated to be $(21.8 \pm 0.4 \pm 0.2)\%$. This result is consistent with the prediction from the statistical isospin model, $\mathcal{B}(\Lambda_c^+ \to \overline{K}^0/K^0 X) = (22.0 \pm 0.7)\%$. The total predicted BF of unseen decays by the statistical isospin model of the inclusive decay $\Lambda_c^+ \to \overline{K}^0/K^0 X$ is $(6.2 \pm 0.4)\%$ as listed in table 1. This is also consistent with the BF of the undiscovered decay channels of Λ_c^+ containing K_S^0 in the final state, estimated from our measured result. It can be seen from table 1 that the predicted undiscovered decay channels are dominated by the decays which contain neutrons in the final state. Due to the challenge of neutron reconstruction, only the BF of $\Lambda_c^+ \to n K_S^0 \pi^+$ has been reported by BESIII [8, 38]. By developing neutron reconstruction techniques [39], the $\Lambda_c^+ \to n \overline{K}^0 \pi^+ \pi^0$ decay, which accounts for almost half of the unobserved decays of $\Lambda_c^+ \to \overline{K}^0/K^0 X$, could be measured. For $\Lambda_c^+ \to \Xi^0 K^0 \pi^+$, the theory based on SU(3) flavor symmetry predicts its BF to be $(8.7 \pm 1.7)\%$ [40], which differs significantly from the estimation by the statistical isospin model, as listed in table 1. Our result disfavors the predictions of SU(3) flavor symmetry indirectly and shows that a direct measurement of the unobserved K_S^0-involved decays of Λ_c^+ is important for further testing the statistical isospin model.

JHEP06(2025)194

Acknowledgments

The BESIII Collaboration thanks the staff of BEPCII and the IHEP computing center for their strong support. This work is supported in part by National Key R&D Program of China under Contracts Nos. 2023YFA1606000, 2023YFA1609400; National Natural Science Foundation of China (NSFC) under Contracts Nos. 12105127, 12305105, 12422504, 11635010, 11735014, 11935015, 11935016, 11935018, 12025502, 12035009, 12035013, 12061131003, 12192260, 12192261, 12192262, 12192263, 12192264, 12192265, 12221005, 12225509, 12235017, 12361141819, 12375092; the Chinese Academy of Sciences (CAS) Large-Scale Scientific Facility Program; the CAS Center for Excellence in Particle Physics (CCEPP); Joint Large-Scale Scientific Facility Funds of the NSFC and CAS under Contract No. U1832207; CAS under Contract No. YSBR-101; 100 Talents Program of CAS; Fundamental Research Funds for the Central Universities, Lanzhou University; The Institute of Nuclear and Particle Physics (INPAC) and Shanghai Key Laboratory for Particle Physics and Cosmology; Agencia Nacional de Investigación y Desarrollo de Chile (ANID), Chile under Contract No. ANID PIA/APOYO AFB230003; German Research Foundation DFG under Contract No. FOR5327; Istituto Nazionale di Fisica Nucleare, Italy; Knut and Alice Wallenberg Foundation under Contracts Nos. 2021.0174, 2021.0299; Ministry of Development of Turkey under Contract No. DPT2006K-120470; National Research Foundation of Korea under Contract No. NRF-2022R1A2C1092335; National Science and Technology fund of Mongolia; National Science Research and Innovation Fund (NSRF) via the Program Management Unit for Human Resources & Institutional Development, Research and Innovation of Thailand under Contract No. B50G670107; Polish National Science Centre under Contract No. 2019/35/O/ST2/02907; Swedish Research Council under Contract No. 2019.04595; The Swedish Foundation for International Cooperation in Research and Higher Education under Contract No. CH2018-7756; U.S. Department of Energy under Contract No. DE-FG02-05ER41374.

Data Availability Statement. This article has no associated data or the data will not be deposited.

Code Availability Statement. This article has no associated code or the code will not be deposited.

References

[1] G.S. Abrams et al., *Observation of Charmed Baryon Production in e^+e^- Annihilation*, *Phys. Rev. Lett.* **44** (1980) 10 [INSPIRE].

[2] BESIII collaboration, *Measurement of the absolute branching fraction for $\Lambda_c^+ \to \Lambda e^+\nu_e$*, *Phys. Rev. Lett.* **115** (2015) 221805 [arXiv:1510.02610] [INSPIRE].

[3] BESIII collaboration, *Measurements of absolute hadronic branching fractions of Λ_c^+ baryon*, *Phys. Rev. Lett.* **116** (2016) 052001 [arXiv:1511.08380] [INSPIRE].

[4] BESIII collaboration, *Measurement of Singly Cabibbo Suppressed Decays* $\Lambda_c^+ \to p\pi^+\pi^-$ *and* $\Lambda_c^+ \to pK^+K^-$, *Phys. Rev. Lett.* **117** (2016) 232002 [*Addendum ibid.* **120** (2018) 029903] [arXiv:1608.00407] [INSPIRE].

[5] BESIII collaboration, *Evidence for the singly-Cabibbo-suppressed decay* $\Lambda_c^+ \to p\eta$ *and search for* $\Lambda_c^+ \to p\pi^0$, *Phys. Rev. D* **95** (2017) 111102 [arXiv:1702.05279] [INSPIRE].

[6] BESIII collaboration, *Measurement of the absolute branching fraction for* $\Lambda_c^+ \to \Lambda\mu^+\nu_\mu$, *Phys. Lett. B* **767** (2017) 42 [arXiv:1611.04382] [INSPIRE].

[7] BESIII collaboration, *Observation of the decay* $\Lambda_c^+ \to \Sigma^-\pi^+\pi^+\pi^0$, *Phys. Lett. B* **772** (2017) 388 [arXiv:1705.11109] [INSPIRE].

[8] BESIII collaboration, *Observation of* $\Lambda_c^+ \to nK_S^0\pi^+$, *Phys. Rev. Lett.* **118** (2017) 112001 [arXiv:1611.02797] [INSPIRE].

[9] BESIII collaboration, *Measurements of absolute branching fractions for* $\Lambda_c^+ \to \Xi^0K^+$ *and* $\Xi(1530)^0K^+$, *Phys. Lett. B* **783** (2018) 200 [arXiv:1803.04299] [INSPIRE].

[10] BESIII collaboration, *Evidence for the decays of* $\Lambda_c^+ \to \Sigma^+\eta$ *and* $\Sigma^+\eta'$, *Chin. Phys. C* **43** (2019) 083002 [arXiv:1811.08028] [INSPIRE].

[11] BESIII collaboration, *Measurement of the absolute branching fractions of* $\Lambda_c^+ \to \Lambda\eta\pi^+$ *and* $\Sigma(1385)^+\eta$, *Phys. Rev. D* **99** (2019) 032010 [arXiv:1812.10731] [INSPIRE].

[12] BESIII collaboration, *Measurement of the absolute branching fraction of* $\Lambda_c^+ \to pK_S^0\eta$ *decays*, *Phys. Lett. B* **817** (2021) 136327 [arXiv:2012.11106] [INSPIRE].

[13] BESIII collaboration, *Observation of the Singly Cabibbo Suppressed Decay* $\Lambda_c^+ \to n\pi^+$, *Phys. Rev. Lett.* **128** (2022) 142001 [arXiv:2201.02056] [INSPIRE].

[14] H.-B. Li and X.-R. Lyu, *Study of the standard model with weak decays of charmed hadrons at BESIII*, *Natl. Sci. Rev.* **8** (2021) nwab181 [arXiv:2103.00908] [INSPIRE].

[15] Particle Data Group collaboration, *Review of particle physics*, *Phys. Rev. D* **110** (2024) 030001 [INSPIRE].

[16] M. Gronau, J.L. Rosner and C.G. Wohl, *Overview of* Λ_c *decays*, *Phys. Rev. D* **97** (2018) 116015 [*Addendum ibid.* **98** (2018) 073003] [arXiv:1808.03720] [INSPIRE].

[17] J.G. Körner, G. Kramer and J. Willrodt, *Weak Decays of the Charmed Baryon* C_0^+ *and the Inclusive Yield of* Λ *and* p, *Phys. Lett. B* **78** (1978) 492 [INSPIRE].

[18] H.-Y. Cheng, *Charmed baryon physics circa 2021*, *Chin. J. Phys.* **78** (2022) 324 [arXiv:2109.01216] [INSPIRE].

[19] J. Gratrex, B. Melić and I. Nišandžić, *Lifetimes of singly charmed hadrons*, *JHEP* **07** (2022) 058 [arXiv:2204.11935] [INSPIRE].

[20] BESIII collaboration, *Measurement of absolute branching fraction of the inclusive decay* $\Lambda_c^+ \to \Lambda + X$, *Phys. Rev. Lett.* **121** (2018) 062003 [arXiv:1803.05706] [INSPIRE].

[21] BESIII collaboration, *Measurement of the absolute branching fraction of the inclusive semileptonic* Λ_c^+ *decay*, *Phys. Rev. Lett.* **121** (2018) 251801 [arXiv:1805.09060] [INSPIRE].

[22] BESIII collaboration, *Measurement of the absolute branching fraction of the inclusive decay* $\Lambda_c^+ \to K_S^0X$, *Eur. Phys. J. C* **80** (2020) 935 [arXiv:2005.11211] [INSPIRE].

[23] BESIII collaboration, *Observations of the Cabibbo-Suppressed decays* $\Lambda_c^+ \to n\pi^+\pi^0$, $n\pi^+\pi^-\pi^+$ *and the Cabibbo-Favored decay* $\Lambda_c^+ \to nK^-\pi^+\pi^+$, *Chin. Phys. C* **47** (2023) 023001 [arXiv:2210.03375] [INSPIRE].

JHEP06(2025)194

[24] MARK-III collaboration, *Observation of a Narrow $K\bar{K}$ State in J/ψ Radiative Decays*, *Phys. Rev. Lett.* **56** (1986) 107 [INSPIRE].

[25] MARK-III collaboration, *Measurement of the branching fractions for $D^0 \to \pi^- e^+ \nu_e$ and $D^0 \to K^- e^+ \nu_e$ and determination of $\|V_{cd}/V_{cs}\|^2$*, *Phys. Rev. Lett.* **62** (1989) 1821 [INSPIRE].

[26] BESIII collaboration, *Design and Construction of the BESIII Detector*, *Nucl. Instrum. Meth. A* **614** (2010) 345 [arXiv:0911.4960] [INSPIRE].

[27] C. Yu et al., *BEPCII Performance and Beam Dynamics Studies on Luminosity*, in the proceedings of the *7th International Particle Accelerator Conference*, Busan, South Korea, May 08–13 (2016) [DOI:10.18429/JACoW-IPAC2016-TUYA01] [INSPIRE].

[28] X. Li et al., *Study of MRPC technology for BESIII endcap-TOF upgrade*, *Radiat. Detect. Technol. Methods* **1** (2017) 13 [INSPIRE].

[29] Y.-X. Guo et al., *The study of time calibration for upgraded end cap TOF of BESIII*, *Radiat. Detect. Technol. Methods* **1** (2017) 15 [INSPIRE].

[30] P. Cao et al., *Design and construction of the new BESIII endcap Time-of-Flight system with MRPC Technology*, *Nucl. Instrum. Meth. A* **953** (2020) 163053 [INSPIRE].

[31] GEANT4 collaboration, *GEANT4 — A Simulation Toolkit*, *Nucl. Instrum. Meth. A* **506** (2003) 250 [INSPIRE].

[32] J. Allison et al., *Geant4 developments and applications*, *IEEE Trans. Nucl. Sci.* **53** (2006) 270 [INSPIRE].

[33] S. Jadach, B.F.L. Ward and Z. Was, *Coherent exclusive exponentiation for precision Monte Carlo calculations*, *Phys. Rev. D* **63** (2001) 113009 [hep-ph/0006359] [INSPIRE].

[34] D.J. Lange, *The EvtGen particle decay simulation package*, *Nucl. Instrum. Meth. A* **462** (2001) 152 [INSPIRE].

[35] R.-G. Ping, *Event generators at BESIII*, *Chin. Phys. C* **32** (2008) 599 [INSPIRE].

[36] J.C. Chen et al., *Event generator for J/ψ and $\psi(2S)$ decay*, *Phys. Rev. D* **62** (2000) 034003 [INSPIRE].

[37] ARGUS collaboration, *Search for Hadronic $b \to u$ Decays*, *Phys. Lett. B* **241** (1990) 278 [INSPIRE].

[38] BESIII collaboration, *Measurement of branching fractions for $\Lambda_c^+ \to nK_S^0\pi^+$ and $\Lambda_c^+ \to nK_S^0K^+$*, *Phys. Rev. D* **109** (2024) 072010 [arXiv:2311.17131] [INSPIRE].

[39] BESIII collaboration, *Observation of a rare beta decay of the charmed baryon with a Graph Neural Network*, *Nature Commun.* **16** (2025) 681 [arXiv:2410.13515] [INSPIRE].

[40] C.-Q. Geng, C.-W. Liu, T.-H. Tsai and Y. Yu, *Charmed Baryon Weak Decays with Decuplet Baryon and $SU(3)$ Flavor Symmetry*, *Phys. Rev. D* **99** (2019) 114022 [arXiv:1904.11271] [INSPIRE].

The BESIII collaboration

M. Ablikim[1], M.N. Achasov[4,c], P. Adlarson[76], X.C. Ai[81], R. Aliberti[35], A. Amoroso[75A,75C], Q. An[72,58,a], Y. Bai[57], O. Bakina[36], Y. Ban[46,h], H.-R. Bao[64], V. Batozskaya[1,44], K. Begzsuren[32], N. Berger[35], M. Berlowski[44], M. Bertani[28A], D. Bettoni[29A], F. Bianchi[75A,75C], E. Bianco[75A,75C], A. Bortone[75A,75C], I. Boyko[36], R.A. Briere[5], A. Brueggemann[69], H. Cai[77], M.H. Cai[38,k,l], X. Cai[1,58], A. Calcaterra[28A], G.F. Cao[1,64], N. Cao[1,64], S.A. Cetin[62A], X.Y. Chai[46,h], J.F. Chang[1,58], G.R. Che[43], Y.Z. Che[1,58,64], G. Chelkov[36,b], C.H. Chen[9], Chao Chen[55], G. Chen[1], H.S. Chen[1,64], H.Y. Chen[20], M.L. Chen[1,58,64], S.J. Chen[42], S.L. Chen[45], S.M. Chen[61], T. Chen[1,64], X.R. Chen[31,64], X.T. Chen[1,64], Y.B. Chen[1,58], Y.Q. Chen[34], Z.J. Chen[25,i], Z.K. Chen[59], S.K. Choi[10], X. Chu[12,g], G. Cibinetto[29A], F. Cossio[75C], J.J. Cui[50], H.L. Dai[1,58], J.P. Dai[79], A. Dbeyssi[18], R. E. de Boer[3], D. Dedovich[36], C.Q. Deng[73], Z.Y. Deng[1], A. Denig[35], I. Denysenko[36], M. Destefanis[75A,75C], F. De Mori[75A,75C], B. Ding[67,1], X.X. Ding[46,h], Y. Ding[34], Y. Ding[40], Y.X. Ding[30], J. Dong[1,58], L.Y. Dong[1,64], M.Y. Dong[1,58,64], X. Dong[77], M.C. Du[1], S.X. Du[81], S.X. Du[12,g], Y.Y. Duan[55], Z.H. Duan[42], P. Egorov[36,b], G.F. Fan[42], J.J. Fan[19], Y.H. Fan[45], J. Fang[59], J. Fang[1,58], S.S. Fang[1,64], W.X. Fang[1], Y.Q. Fang[1,58], R. Farinelli[29A], L. Fava[75B,75C], F. Feldbauer[3], G. Felici[28A], C.Q. Feng[72,58], J.H. Feng[59], Y.T. Feng[72,58], M. Fritsch[3], C.D. Fu[1], J.L. Fu[64], Y.W. Fu[1,64], H. Gao[64], X.B. Gao[41], Y.N. Gao[46,h], Y.N. Gao[19], Y.Y. Gao[30], Yang Gao[72,58], S. Garbolino[75C], I. Garzia[29A,29B], P.T. Ge[19], Z.W. Ge[42], C. Geng[59], E.M. Gersabeck[68], A. Gilman[70], K. Goetzen[13], J.D. Gong[34], L. Gong[40], W.X. Gong[1,58], W. Gradl[35], S. Gramigna[29A,29B], M. Greco[75A,75C], M.H. Gu[1,58], Y.T. Gu[15], C.Y. Guan[1,64], A.Q. Guo[31], L.B. Guo[41], M.J. Guo[50], R.P. Guo[49], Y.P. Guo[12,g], A. Guskov[36,b], J. Gutierrez[27], K.L. Han[64], T.T. Han[1], F. Hanisch[3], K.D. Hao[72,58], X.Q. Hao[19], F.A. Harris[66], K.K. He[55], K.L. He[1,64], F.H. Heinsius[3], C.H. Heinz[35], Y.K. Heng[1,58,64], C. Herold[60], T. Holtmann[3], P.C. Hong[34], G.Y. Hou[1,64], X.T. Hou[1,64], Y.R. Hou[64], Z.L. Hou[1], B.Y. Hu[59], H.M. Hu[1,64], J.F. Hu[56,j], Q.P. Hu[72,58], S.L. Hu[12,g], T. Hu[1,58,64], Y. Hu[1], Z.M. Hu[59], G.S. Huang[72,58], K.X. Huang[59], L.Q. Huang[31,64], P. Huang[42], X.T. Huang[50], Y.P. Huang[1], Y.S. Huang[59], T. Hussain[74], N. Hüsken[35], N. in der Wiesche[69], J. Jackson[27], S. Janchiv[32], Q. Ji[1], Q.P. Ji[19], W. Ji[1,64], X.B. Ji[1,64], X.L. Ji[1,58], Y.Y. Ji[50], Z.K. Jia[72,58], D. Jiang[1,64], H.B. Jiang[77], P.C. Jiang[46,h], S.J. Jiang[9], T.J. Jiang[16], X.S. Jiang[1,58,64], Y. Jiang[64], J.B. Jiao[50], J.K. Jiao[34], Z. Jiao[23], S. Jin[42], Y. Jin[67], M.Q. Jing[1,64], X.M. Jing[64], T. Johansson[76], S. Kabana[33], N. Kalantar-Nayestanaki[65], X.L. Kang[9], X.S. Kang[40], M. Kavatsyuk[65], B.C. Ke[81], V. Khachatryan[27], A. Khoukaz[69], R. Kiuchi[1], O.B. Kolcu[62A], B. Kopf[3], M. Kuessner[3], X. Kui[1,64], N. Kumar[26], A. Kupsc[44,76], W. Kühn[37], Q. Lan[73], W.N. Lan[19], T.T. Lei[72,58], M. Lellmann[35], T. Lenz[35], C. Li[43], C. Li[47], C.H. Li[39], C.K. Li[20], Cheng Li[72,58], D.M. Li[81], F. Li[1,58], G. Li[1], H.B. Li[1,64], H.J. Li[19], H.N. Li[56,j], Hui Li[43], J.R. Li[61], J.S. Li[59], K. Li[1], K.L. Li[19], K.L. Li[38,k,l], L.J. Li[1,64], Lei Li[48], M.H. Li[43], M.R. Li[1,64], P.L. Li[64], P.R. Li[38,k,l], Q.M. Li[1,64], Q.X. Li[50], R. Li[17,31], T. Li[50], T.Y. Li[43], W.D. Li[1,64], W.G. Li[1,a], X. Li[1,64], X.H. Li[72,58], X.L. Li[50], X.Y. Li[1,8], X.Z. Li[59], Y. Li[19], Y.G. Li[46,h], Y.P. Li[34], Z.J. Li[59], Z.Y. Li[79], C. Liang[42], H. Liang[72,58], Y.F. Liang[54], Y.T. Liang[31,64], G.R. Liao[14], L.B. Liao[59], M.H. Liao[59], Y.P. Liao[1,64], J. Libby[26], A. Limphirat[60], C.C. Lin[55], C.X. Lin[64], D.X. Lin[31,64], L.Q. Lin[39], T. Lin[1], B.J. Liu[1], B.X. Liu[77], C. Liu[34], C.X. Liu[1], F. Liu[1], F.H. Liu[53], Feng Liu[6], G.M. Liu[56,j], H. Liu[38,k,l], H.B. Liu[15], H.H. Liu[1], H.M. Liu[1,64], Huihui Liu[21], J.B. Liu[72,58], J.J. Liu[20], K. Liu[38,k,l], K. Liu[73], K.Y. Liu[40], Ke Liu[22], L. Liu[72,58], L.C. Liu[43], Lu Liu[43], P.L. Liu[1], Q. Liu[64], S.B. Liu[72,58], T. Liu[12,g], W.K. Liu[43], W.M. Liu[72,58], W.T. Liu[39], X. Liu[39], X. Liu[38,k,l], X.Y. Liu[77], Y. Liu[38,k,l], Y. Liu[81], Y. Liu[81], Y.B. Liu[43], Z.A. Liu[1,58,64], Z.D. Liu[9], Z.Q. Liu[50], X.C. Lou[1,58,64], F.X. Lu[59], H.J. Lu[23],

JHEP06(2025)194

J.G. Lu[1,58], Y. Lu[7], Y.H. Lu[1,64], Y.P. Lu[1,58], Z.H. Lu[1,64], C.L. Luo[41], J.R. Luo[59], J.S. Luo[1,64], M.X. Luo[80], T. Luo[12,g], X.L. Luo[1,58], Z.Y. Lv[22], X.R. Lyu[64,p], Y.F. Lyu[43], Y.H. Lyu[81], F.C. Ma[40], H. Ma[79], H.L. Ma[1], J.L. Ma[1,64], L.L. Ma[50], L.R. Ma[67], Q.M. Ma[1], R.Q. Ma[1,64], R.Y. Ma[19], T. Ma[72,58], X.T. Ma[1,64], X.Y. Ma[1,58], Y.M. Ma[31], F.E. Maas[18], I. MacKay[70], M. Maggiora[75A,75C], S. Malde[70], Y.J. Mao[46,h], Z.P. Mao[1], S. Marcello[75A,75C], F.M. Melendi[29A,29B], Y.H. Meng[64], Z.X. Meng[67], J.G. Messchendorp[13,65], G. Mezzadri[29A], H. Miao[1,64], T.J. Min[42], R.E. Mitchell[27], X.H. Mo[1,58,64], B. Moses[27], N. Yu. Muchnoi[4,c], J. Muskalla[35], Y. Nefedov[36], F. Nerling[18,e], L.S. Nie[20], I.B. Nikolaev[4,c], Z. Ning[1,58], S. Nisar[11,m], Q.L. Niu[38,k,l], W.D. Niu[12,g], S.L. Olsen[10,64], Q. Ouyang[1,58,64], S. Pacetti[28B,28C], X. Pan[55], Y. Pan[57], A. Pathak[10], Y.P. Pei[72,58], M. Pelizaeus[3], H.P. Peng[72,58], Y.Y. Peng[38,k,l], K. Peters[13,e], J.L. Ping[41], R.G. Ping[1,64], S. Plura[35], V. Prasad[33], F.Z. Qi[1], H.R. Qi[61], M. Qi[42], S. Qian[1,58], W.B. Qian[64], C.F. Qiao[64], J.H. Qiao[19], J.J. Qin[73], J.L. Qin[55], L.Q. Qin[14], L.Y. Qin[72,58], P.B. Qin[73], X.P. Qin[12,g], X.S. Qin[50], Z.H. Qin[1,58], J.F. Qiu[1], Z.H. Qu[73], C.F. Redmer[35], A. Rivetti[75C], M. Rolo[75C], G. Rong[1,64], S.S. Rong[1,64], F. Rosini[28B,28C], Ch. Rosner[18], M.Q. Ruan[1,58], N. Salone[44], A. Sarantsev[36,d], Y. Schelhaas[35], K. Schoenning[76], M. Scodeggio[29A], K.Y. Shan[12,g], W. Shan[24], X.Y. Shan[72,58], Z.J. Shang[38,k,l], J.F. Shangguan[16], L.G. Shao[1,64], M. Shao[72,58], C.P. Shen[12,g], H.F. Shen[1,8], W.H. Shen[64], X.Y. Shen[1,64], B.A. Shi[64], H. Shi[72,58], J.L. Shi[12,g], J.Y. Shi[1], S.Y. Shi[73], X. Shi[1,58], H.L. Song[72,58], J.J. Song[19], T.Z. Song[59], W.M. Song[34,1], Y.X. Song[46,h,n], S. Sosio[75A,75C], S. Spataro[75A,75C], F. Stieler[35], S. S Su[40], Y.J. Su[64], G.B. Sun[77], G.X. Sun[1], H. Sun[64], H.K. Sun[1], J.F. Sun[19], K. Sun[61], L. Sun[77], S.S. Sun[1,64], T. Sun[51,f], Y.C. Sun[77], Y.H. Sun[30], Y.J. Sun[72,58], Y.Z. Sun[1], Z.Q. Sun[1,64], Z.T. Sun[50], C.J. Tang[54], G.Y. Tang[1], J. Tang[59], L.F. Tang[39], M. Tang[72,58], Y.A. Tang[77], L.Y. Tao[73], M. Tat[70], J.X. Teng[72,58], J.Y. Tian[72,58], W.H. Tian[59], Y. Tian[31], Z.F. Tian[77], I. Uman[62B], B. Wang[1], B. Wang[59], Bo Wang[72,58], C. Wang[19], Cong Wang[22], D.Y. Wang[46,h], H.J. Wang[38,k,l], J.J. Wang[77], K. Wang[1,58], L.L. Wang[1], L.W. Wang[34], M. Wang[50], M. Wang[72,58], N.Y. Wang[64], S. Wang[12,g], T. Wang[12,g], T.J. Wang[43], W. Wang[73], W. Wang[59], W.P. Wang[35,58,72,o], X. Wang[46,h], X.F. Wang[38,k,l], X.J. Wang[39], X.L. Wang[12,g], X.N. Wang[1], Y. Wang[61], Y.D. Wang[45], Y.F. Wang[1,58,64], Y.H. Wang[38,k,l], Y.L. Wang[19], Y.N. Wang[77], Y.Q. Wang[1], Yaqian Wang[17], Yi Wang[61], Yuan Wang[17,31], Z. Wang[1,58], Z.L. Wang[2], Z.L. Wang[73], Z.Q. Wang[12,g], Z.Y. Wang[1,64], D.H. Wei[14], H.R. Wei[43], F. Weidner[69], S.P. Wen[1], Y.R. Wen[39], U. Wiedner[3], G. Wilkinson[70], M. Wolke[76], C. Wu[39], J.F. Wu[1,8], L.H. Wu[1], L.J. Wu[1,64], Lianjie Wu[19], S.G. Wu[1,64], S.M. Wu[64], X. Wu[12,g], X.H. Wu[34], Y.J. Wu[31], Z. Wu[1,58], L. Xia[72,58], X.M. Xian[39], B.H. Xiang[1,64], T. Xiang[46,h], D. Xiao[38,k,l], G.Y. Xiao[42], H. Xiao[73], Y. L. Xiao[12,g], Z.J. Xiao[41], C. Xie[42], K.J. Xie[1,64], X.H. Xie[46,h], Y. Xie[50], Y.G. Xie[1,58], Y.H. Xie[6], Z.P. Xie[72,58], T.Y. Xing[1,64], C.F. Xu[1,64], C.J. Xu[59], G.F. Xu[1], H.Y. Xu[2], H.Y. Xu[67,2], M. Xu[72,58], Q.J. Xu[16], Q.N. Xu[30], W.L. Xu[67], X.P. Xu[55], Y. Xu[40], Y. Xu[12,g], Y.C. Xu[78], Z.S. Xu[64], H.Y. Yan[39], L. Yan[12,g], W.B. Yan[72,58], W.C. Yan[81], W.P. Yan[19], X.Q. Yan[1,64], H.J. Yang[51,f], H.L. Yang[34], H.X. Yang[1], J.H. Yang[42], R.J. Yang[19], T. Yang[1], Y. Yang[12,g], Y.F. Yang[43], Y.H. Yang[42], Y.Q. Yang[9], Y.X. Yang[1,64], Y.Z. Yang[19], M. Ye[1,58], M.H. Ye[8], Junhao Yin[43], Z.Y. You[59], B.X. Yu[1,58,64], C.X. Yu[43], G. Yu[13], J.S. Yu[25,i], M.C. Yu[40], T. Yu[73], X.D. Yu[46,h], Y.C. Yu[81], C.Z. Yuan[1,64], H. Yuan[1,64], J. Yuan[34], J. Yuan[45], L. Yuan[2], S.C. Yuan[1,64], Y. Yuan[1,64], Z.Y. Yuan[59], C.X. Yue[39], Ying Yue[19], A.A. Zafar[74], S.H. Zeng[63], X. Zeng[12,g], Y. Zeng[25,i], Y.J. Zeng[1,64], Y.J. Zeng[59], X.Y. Zhai[34], Y.H. Zhan[59], A.Q. Zhang[1,64], B.L. Zhang[1,64], B.X. Zhang[1], D.H. Zhang[43], G.Y. Zhang[1,64], G.Y. Zhang[19], H. Zhang[81], H. Zhang[72,58], H.C. Zhang[1,58,64], H.H. Zhang[59], H.Q. Zhang[1,58,64], H.R. Zhang[72,58], H.Y. Zhang[1,58], J. Zhang[81],

JHEP06(2025)194

J. Zhang[59], J.J. Zhang[52], J.L. Zhang[20], J.Q. Zhang[41], J.S. Zhang[12,g], J.W. Zhang[1,58,64], J.X. Zhang[38,k,l], J.Y. Zhang[1], J.Z. Zhang[1,64], Jianyu Zhang[64], L.M. Zhang[61], Lei Zhang[42], N. Zhang[81], P. Zhang[1,64], Q. Zhang[19], Q.Y. Zhang[34], R.Y. Zhang[38,k,l], S.H. Zhang[1,64], Shulei Zhang[25,i], X.M. Zhang[1], X. Y Zhang[40], X.Y. Zhang[50], Y. Zhang[73], Y. Zhang[1], Y. T. Zhang[81], Y.H. Zhang[1,58], Y.M. Zhang[39], Z.D. Zhang[1], Z.H. Zhang[1], Z.L. Zhang[34], Z.L. Zhang[55], Z.X. Zhang[19], Z.Y. Zhang[43], Z.Y. Zhang[77], Z.Z. Zhang[45], Zh. Zh. Zhang[19], G. Zhao[1], J.Y. Zhao[1,64], J.Z. Zhao[1,58], L. Zhao[1], Lei Zhao[72,58], M.G. Zhao[43], N. Zhao[79], R.P. Zhao[64], S.J. Zhao[81], Y.B. Zhao[1,58], Y.L. Zhao[55], Y.X. Zhao[31,64], Z.G. Zhao[72,58], A. Zhemchugov[36,b], B. Zheng[73], B.M. Zheng[34], J.P. Zheng[1,58], W.J. Zheng[1,64], X.R. Zheng[19], Y.H. Zheng[64,p], B. Zhong[41], X. Zhong[59], H. Zhou[35,50,o], J.Q. Zhou[34], J.Y. Zhou[34], S. Zhou[6], X. Zhou[77], X.K. Zhou[6], X.R. Zhou[72,58], X.Y. Zhou[39], Y.Z. Zhou[12,g], Z.C. Zhou[20], A.N. Zhu[64], J. Zhu[43], K. Zhu[1], K.J. Zhu[1,58,64], K.S. Zhu[12,g], L. Zhu[34], L.X. Zhu[64], S.H. Zhu[71], T.J. Zhu[12,g], W.D. Zhu[41], W.D. Zhu[12,g], W.J. Zhu[1], W.Z. Zhu[19], Y.C. Zhu[72,58], Z.A. Zhu[1,64], X.Y. Zhuang[43], J.H. Zou[1], J. Zu[72,58]

[1] *Institute of High Energy Physics, Beijing 100049, People's Republic of China*
[2] *Beihang University, Beijing 100191, People's Republic of China*
[3] *Bochum Ruhr-University, D-44780 Bochum, Germany*
[4] *Budker Institute of Nuclear Physics SB RAS (BINP), Novosibirsk 630090, Russia*
[5] *Carnegie Mellon University, Pittsburgh, Pennsylvania 15213, U.S.A.*
[6] *Central China Normal University, Wuhan 430079, People's Republic of China*
[7] *Central South University, Changsha 410083, People's Republic of China*
[8] *China Center of Advanced Science and Technology, Beijing 100190, People's Republic of China*
[9] *China University of Geosciences, Wuhan 430074, People's Republic of China*
[10] *Chung-Ang University, Seoul, 06974, Republic of Korea*
[11] *COMSATS University Islamabad, Lahore Campus, Defence Road, Off Raiwind Road, 54000 Lahore, Pakistan*
[12] *Fudan University, Shanghai 200433, People's Republic of China*
[13] *GSI Helmholtzcentre for Heavy Ion Research GmbH, D-64291 Darmstadt, Germany*
[14] *Guangxi Normal University, Guilin 541004, People's Republic of China*
[15] *Guangxi University, Nanning 530004, People's Republic of China*
[16] *Hangzhou Normal University, Hangzhou 310036, People's Republic of China*
[17] *Hebei University, Baoding 071002, People's Republic of China*
[18] *Helmholtz Institute Mainz, Staudinger Weg 18, D-55099 Mainz, Germany*
[19] *Henan Normal University, Xinxiang 453007, People's Republic of China*
[20] *Henan University, Kaifeng 475004, People's Republic of China*
[21] *Henan University of Science and Technology, Luoyang 471003, People's Republic of China*
[22] *Henan University of Technology, Zhengzhou 450001, People's Republic of China*
[23] *Huangshan College, Huangshan 245000, People's Republic of China*
[24] *Hunan Normal University, Changsha 410081, People's Republic of China*
[25] *Hunan University, Changsha 410082, People's Republic of China*
[26] *Indian Institute of Technology Madras, Chennai 600036, India*
[27] *Indiana University, Bloomington, Indiana 47405, U.S.A.*
[28] *INFN Laboratori Nazionali di Frascati, (A) INFN Laboratori Nazionali di Frascati, I-00044, Frascati, Italy; (B) INFN Sezione di Perugia, I-06100, Perugia, Italy; (C) University of Perugia, I-06100, Perugia, Italy*
[29] *INFN Sezione di Ferrara, (A)INFN Sezione di Ferrara, I-44122, Ferrara, Italy; (B)University of Ferrara, I-44122, Ferrara, Italy*
[30] *Inner Mongolia University, Hohhot 010021, People's Republic of China*
[31] *Institute of Modern Physics, Lanzhou 730000, People's Republic of China*
[32] *Institute of Physics and Technology, Peace Avenue 54B, Ulaanbaatar 13330, Mongolia*
[33] *Instituto de Alta Investigación, Universidad de Tarapacá, Casilla 7D, Arica 1000000, Chile*

JHEP06(2025)194

[34] *Jilin University, Changchun 130012, People's Republic of China*
[35] *Johannes Gutenberg University of Mainz, Johann-Joachim-Becher-Weg 45, D-55099 Mainz, Germany*
[36] *Joint Institute for Nuclear Research, 141980 Dubna, Moscow region, Russia*
[37] *Justus-Liebig-Universitaet Giessen, II. Physikalisches Institut, Heinrich-Buff-Ring 16, D-35392 Giessen, Germany*
[38] *Lanzhou University, Lanzhou 730000, People's Republic of China*
[39] *Liaoning Normal University, Dalian 116029, People's Republic of China*
[40] *Liaoning University, Shenyang 110036, People's Republic of China*
[41] *Nanjing Normal University, Nanjing 210023, People's Republic of China*
[42] *Nanjing University, Nanjing 210093, People's Republic of China*
[43] *Nankai University, Tianjin 300071, People's Republic of China*
[44] *National Centre for Nuclear Research, Warsaw 02-093, Poland*
[45] *North China Electric Power University, Beijing 102206, People's Republic of China*
[46] *Peking University, Beijing 100871, People's Republic of China*
[47] *Qufu Normal University, Qufu 273165, People's Republic of China*
[48] *Renmin University of China, Beijing 100872, People's Republic of China*
[49] *Shandong Normal University, Jinan 250014, People's Republic of China*
[50] *Shandong University, Jinan 250100, People's Republic of China*
[51] *Shanghai Jiao Tong University, Shanghai 200240, People's Republic of China*
[52] *Shanxi Normal University, Linfen 041004, People's Republic of China*
[53] *Shanxi University, Taiyuan 030006, People's Republic of China*
[54] *Sichuan University, Chengdu 610064, People's Republic of China*
[55] *Soochow University, Suzhou 215006, People's Republic of China*
[56] *South China Normal University, Guangzhou 510006, People's Republic of China*
[57] *Southeast University, Nanjing 211100, People's Republic of China*
[58] *State Key Laboratory of Particle Detection and Electronics, Beijing 100049, Hefei 230026, People's Republic of China*
[59] *Sun Yat-Sen University, Guangzhou 510275, People's Republic of China*
[60] *Suranaree University of Technology, University Avenue 111, Nakhon Ratchasima 30000, Thailand*
[61] *Tsinghua University, Beijing 100084, People's Republic of China*
[62] *Turkish Accelerator Center Particle Factory Group, (A)Istinye University, 34010, Istanbul, Turkey; (B)Near East University, Nicosia, North Cyprus, 99138, Mersin 10, Turkey*
[63] *University of Bristol, H.H. Wills Physics Laboratory, Tyndall Avenue, Bristol, BS8 1TL, U.K.*
[64] *University of Chinese Academy of Sciences, Beijing 100049, People's Republic of China*
[65] *University of Groningen, NL-9747 AA Groningen, The Netherlands*
[66] *University of Hawaii, Honolulu, Hawaii 96822, U.S.A.*
[67] *University of Jinan, Jinan 250022, People's Republic of China*
[68] *University of Manchester, Oxford Road, Manchester, M13 9PL, United Kingdom*
[69] *University of Muenster, Wilhelm-Klemm-Strasse 9, 48149 Muenster, Germany*
[70] *University of Oxford, Keble Road, Oxford OX13RH, United Kingdom*
[71] *University of Science and Technology Liaoning, Anshan 114051, People's Republic of China*
[72] *University of Science and Technology of China, Hefei 230026, People's Republic of China*
[73] *University of South China, Hengyang 421001, People's Republic of China*
[74] *University of the Punjab, Lahore-54590, Pakistan*
[75] *University of Turin and INFN, (A) University of Turin, I-10125, Turin, Italy; (B) University of Eastern Piedmont, I-15121, Alessandria, Italy; (C) INFN, I-10125, Turin, Italy*
[76] *Uppsala University, Box 516, SE-75120 Uppsala, Sweden*
[77] *Wuhan University, Wuhan 430072, People's Republic of China*
[78] *Yantai University, Yantai 264005, People's Republic of China*
[79] *Yunnan University, Kunming 650500, People's Republic of China*
[80] *Zhejiang University, Hangzhou 310027, People's Republic of China*
[81] *Zhengzhou University, Zhengzhou 450001, People's Republic of China*

JHEP06(2025)194

[a] *Deceased*
[b] *Also at the Moscow Institute of Physics and Technology, Moscow 141700, Russia*
[c] *Also at the Novosibirsk State University, Novosibirsk, 630090, Russia*
[d] *Also at the NRC "Kurchatov Institute", PNPI, 188300, Gatchina, Russia*
[e] *Also at Goethe University Frankfurt, 60323 Frankfurt am Main, Germany*
[f] *Also at Key Laboratory for Particle Physics, Astrophysics and Cosmology, Ministry of Education; Shanghai Key Laboratory for Particle Physics and Cosmology; Institute of Nuclear and Particle Physics, Shanghai 200240, People's Republic of China*
[g] *Also at Key Laboratory of Nuclear Physics and Ion-beam Application (MOE) and Institute of Modern Physics, Fudan University, Shanghai 200443, People's Republic of China*
[h] *Also at State Key Laboratory of Nuclear Physics and Technology, Peking University, Beijing 100871, People's Republic of China*
[i] *Also at School of Physics and Electronics, Hunan University, Changsha 410082, China*
[j] *Also at Guangdong Provincial Key Laboratory of Nuclear Science, Institute of Quantum Matter, South China Normal University, Guangzhou 510006, China*
[k] *Also at MOE Frontiers Science Center for Rare Isotopes, Lanzhou University, Lanzhou 730000, People's Republic of China*
[l] *Also at Lanzhou Center for Theoretical Physics, Lanzhou University, Lanzhou 730000, People's Republic of China*
[m] *Also at the Department of Mathematical Sciences, IBA, Karachi 75270, Pakistan*
[n] *Also at Ecole Polytechnique Federale de Lausanne (EPFL), CH-1015 Lausanne, Switzerland*
[o] *Also at Helmholtz Institute Mainz, Staudinger Weg 18, D-55099 Mainz, Germany*
[p] *Also at Hangzhou Institute for Advanced Study, University of Chinese Academy of Sciences, Hangzhou 310024, China*

JHEP06(2025)194